Available online at www.sciencedirect.com

ScienceDirect

Ceramics International 40 (2014) 3215–3220

CERAMICS INTERNATIONAL

www.elsevier.com/locate/ceramint

The influence of oxygen partial pressure on the performance and stability of Ge-doped InGaO thin film transistors

Kwang-Ho Lee[a], Kyung-Chul Ok[a], H. Kim[b,*], Jin-Seong Park[a,*]

[a]Division of Materials Science and Engineering, Hanyang University, 222 Wangsimni-ro, Seoul 133-719, Republic of Korea
[b]Department of Materials Science and Engineering, Korea Advanced Institute of Science and Tehcnology, Taejeon, Republic of Korea

Received 3 September 2013; received in revised form 24 September 2013; accepted 26 September 2013
Available online 4 October 2013

Abstract

The device performance and bias stability of radio frequency (RF) sputtered Ge-doped InGaO (GIGO) thin film transistors (TFTs) were investigated as a function of oxygen partial pressure during the deposition step. At low oxygen partial pressure, the electrical performance and stability of GIGO TFTs were significantly improved with a decrease of oxygen deficient bonding states, suggesting strong oxygen bonding ability of Ge atoms. We demonstrate that these changes can be corroborated with the evolution of the electronic structure, such as band alignment and band edge states below the conduction band, as measured by X-ray photoelectron spectroscopy and spectroscopic ellipsometry analysis. As the oxygen partial pressure decreased, the energy difference between the conduction band minimum and Fermi level and the deep band edge states was decreased. In particular, it was revealed that, with an increase of oxygen partial pressure, the relative energy level of the band edge states was shifted to a deeper level within the bandgap.

Keywords: Oxide semiconductor; Thin film transistor; Ge–In–Ga–O; Oxygen pressure; Bias stability

1. Introduction

Amorphous oxide semiconductor-based thin film transistors (AOS-TFTs) have been extensively studied for applications in backplane electronic devices such as active-matrix liquid crystal displays (AMLCDs) and organic light-emitting diodes (AMOLEDs) due to their high field effect mobility, good gate swing, low temperature processing capability, and transparency to visible light [1–4]. Following Hosono et al.'s report on amorphous indium–gallium–zinc oxide TFTs with promising device performance, various oxide semiconductors based on indium, zinc, and tin oxide compounds have been intensively studied [3].

However, in terms of practical mass production, the fabrication of AOS-TFTs with higher device performance and better device stability remains the most important issue. Recently, a great deal of effort has been placed on searching for alternative oxide semiconductors with excellent stability under bias and illumination stress, mainly through the use of a combinatorial material design approach [5,6]. In addition, various oxide semiconductors have been investigated as a TFT channel layer to enhance the TFT characteristics by controlling the carrier concentration and mobility. Several research groups have also studied optimization of the device structure, materials, and process parameters in order to understand and thereupon address the degradation of device performance and stability [7–9]. While previous reports have suggested that the device operation and stress induced device instabilities are predominantly due to the charge trapping mechanism related to oxygen defects, the origins and interpretations of device instability remain unclear [10,11]. More detailed and systematic approaches in terms of elucidating the electronic structure of oxide semiconductors are thus necessary, because it may be strongly related to the charge transport and trapping behaviors, which influence the device characteristics.

In the present work, device performance and bias instability of Ge-doped InGaO (GIGO) oxide TFTs (where the role of Ge

*Corresponding authors.
E-mail addresses: hkim_2@naver.com (H. Kim), jsparklime@hanyang.ac.kr (J.-S. Park).

0272-8842/$ - see front matter © 2013 Elsevier Ltd and Techna Group S.r.l. All rights reserved.
http://dx.doi.org/10.1016/j.ceramint.2013.09.118

is to control the net electron carrier concentration by suppressing carrier generation via oxygen vacancy formation) are investigated as a function of RF-sputtered oxygen pressure, with respect to the electronic structure of band alignment and band edge states below the conduction band, which are also correlated to the chemical bonding states. It was found that a GIGO active layer deposited under lower oxygen partial pressure exhibits better device characteristics, with reduced oxygen deficient chemical bonding states and deep band edge states.

2. Experiment

A heavily doped p-type Si wafer with a thermally grown SiO_2 (100 nm) wafer was used as a substrate onto which GIGO films were deposited using a single ceramic target (with a composition of Ge_2O_3:In_2O_3:Ga_2O_3=1:7:2 mol%), without substrate heating, by a radio frequency (RF) sputtering system. The RF power and oxygen partial pressure [O_2/(O_2+Ar)] were set to 75 W and changed from 2% to 20%, respectively. The active area was defined using a shadow mask during GIGO film deposition. The indium–tin-oxide (ITO) source/drain (S/D) electrode was then deposited and patterned again using shadow masks. The fabricated TFTs had a bottom gate structure, and a channel width (W) and length (L) of 1000 μm and 150 μm, respectively. Finally, GIGO TFTs were annealed at 350 °C for 1 h, by using a furnace system. In order to analyze the physical and electronic properties of GIGO films, separated GIGO films were prepared on identical substrates and subjected to the same heat treatments as for the TFT devices. Regardless of the oxygen partial pressure, the

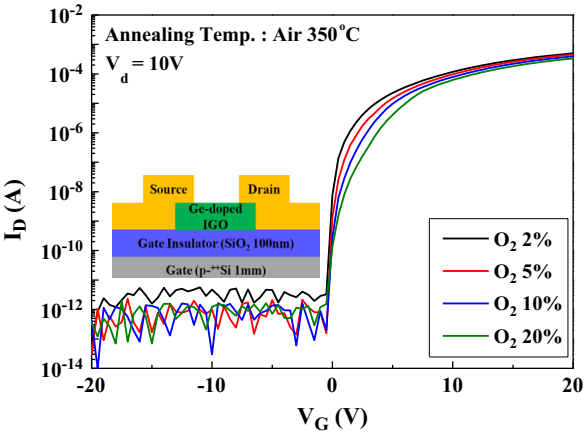

Fig. 1. Representative transfer characteristics of GIGO TFTs as a function of the oxygen partial pressure and schematic diagram of GIGO TFTs (inset).

film composition, investigated by Rutherford backscattering spectroscopy (RBS), was ~10% Ge doping into InGaO, and the physical structure, measured by X-ray diffraction (XRD), was preserved as an amorphous structure. Chemical bonding states were also examined by X-ray photoelectron spectroscopy (XPS), using a monochromatic AlKa source, with a pass energy of 20 eV. The electronic structures, which are related to changes in band alignment and band edge states below the conduction band, were investigated by XPS and spectroscopic ellipsometry (SE). The SE measurements were performed by a rotating analyzer system with an auto retarder in an energy range of 0.75–6.4 eV with incident angles of 65°, 70°, and 75°.

3. Results and discussion

Fig. 1 shows the representative transfer characteristics of the TFTs with the GIGO active layer deposited under different oxygen partial pressures of 2%, 5%, 10%, and 20%. The field effect mobility (μ_{FE}) and threshold voltage (V_{th}) in the saturation region (V_{DS} = 10.1 V) were calculated by fitting a straight line to the plot of the square root of I_{DS} vs. V_{GS}, according to the expression for a field-effect transistor [12]. The subthreshold gate swing (SS) value was extracted from the linear part of the log(I_{DS}) vs. V_{GS} plot [13]. A significant improvement of the device performance was observed for the TFTs with the GIGO active layer deposited under an oxygen partial process pressure of 2%, and the detailed device parameters are summarized in Table 1. As the oxygen partial pressure decreased from 20% to 2%, the μ_{FE} and SS values in GIGO TFTs significantly improved, from 11.33 cm^2/V s and 0.29 V/decade to 14.46 cm^2/V s and 0.12 V/decade, respectively. These results suggest that the oxygen partial pressure is a critical factor in controlling the charge-trapped defects in the GIGO semiconductor and/or interface (GIGO/SiO_2), due to improved mobility and SS values [14].

The RBS analysis revealed that the oxygen composition of the GIGO film slightly increased from 61.1% to 63.1%, as the oxygen partial pressure increased from 2% to 20%. However, the indium (In) element in GGIO films slightly decreased from 22.2% to 21.1% without altering other elements (Ga and Ge). Generally, it is quite reasonable to assume that higher oxygen partial pressure would lead to greater incorporation of oxygen element into the GIGO film. Thus, the compositional change of In and oxygen elements can affect the mobility and oxygen-related defects.

Fig. 2 depicts the crystallinity of the GIGO films after 350 °C annealing. All films have an amorphous structure independent of the oxygen partial pressures. This suggests

Table 1
Comparison of various device parameters of GIGO TFTs as a function of the oxygen partial pressure.

	V_{th} (V)	Mobility (cm^2/V s)	SS (V/decade)	On/off ratio	Hysteresis (V)
O_2 2%	1.50	14.46	0.12	2.47E+10	0.13
O_2 5%	1.97	13.93	0.13	3.09E+09	0.22
O_2 10%	2.40	12.59	0.21	1.32E+10	0.35
O_2 20%	2.60	11.33	0.29	8.44E+09	0.71

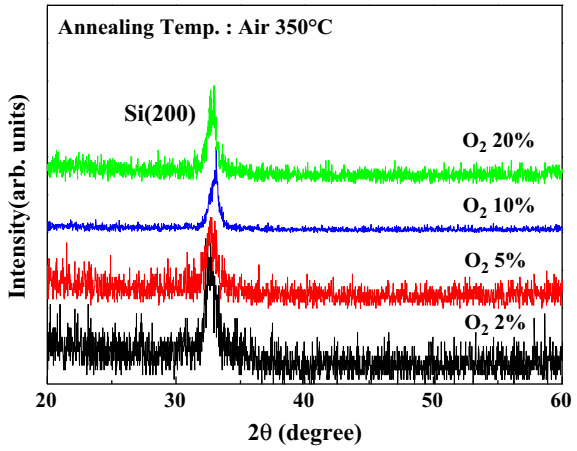

Fig. 2. The XRD peaks of GIGO films depending on oxygen partial pressure, after 350 °C annealing.

that the differences in the GIGO TFT performances did not originate from physical structures.

The bias instability of the TFTs with GIGO active layers was also investigated as a function of oxygen partial pressure under a positive bias stress (PBS) condition, with a gate bias of +20 V after 0, 33, 100, 316, 1000, and 3000 s, as shown in Fig. 3. As the stress time lapses, the transfer characteristics of the GIGO TFTs systematically shift in the positive direction, without any significant changes of the mobility and SS values [see Fig. 3(a)]. It is noted that the TFT with higher oxygen pressure exhibits a larger shift in the positive direction of the transfer curve. The V_{th} of the TFT at $pO_2=20\%$ shifts by +4.68 V, while that at $pO_2=2\%$ exhibited only a +1.12 V shift in V_{th}. The SS value of a given TFT device is related to the total trap density, including the bulk (N_{SS}) and semiconductor–insulator interfacial traps (D_{it}) [15], according to Eq. (1)

$$SS = \frac{qk_BT(N_{SS}t_{ch}+D_{it})}{C_i \log(e)} \quad (1)$$

where q is the electron charge, k_B is Boltzmann's constant, T is the absolute temperature, and t_{ch} is the channel layer thickness. N_{SS} and D_{it} in the GIGO TFTs were calculated by setting one of the parameters to zero. In the present study, the N_{SS} and D_{it} values correspond to the maximum trap density that can be formed in a given system. For example, the N_{SS} and D_{it} values for the GIGO device at $pO_2=20\%$ were 3.6×10^{17} eV^{-1} cm^3 and 1.1×10^{12} eV^{-1} cm^{-2}, respectively. For the device at $pO_2=2\%$, these values decreased considerably to 1.5×10^{17} eV^{-1} cm^3 and 4.5×10^{11} eV^{-1} cm^{-2}, respectively. The decrease in the trap density is consistent with the reduction of the hysteresis of transfer characteristics from 0.71 V to 0.13 V. Therefore, the improvement in PBS instability with a decrease of the oxygen partial pressure is attributed to the reduced N_{SS} and/or D_{it} because electron carrier trapping is directly proportional to the total number of available trap states at the GIGO interface and bulk region. In order to understand the detailed mechanism underlying device performance and instability in GIGO TFTs, more discussion is provided below, mainly

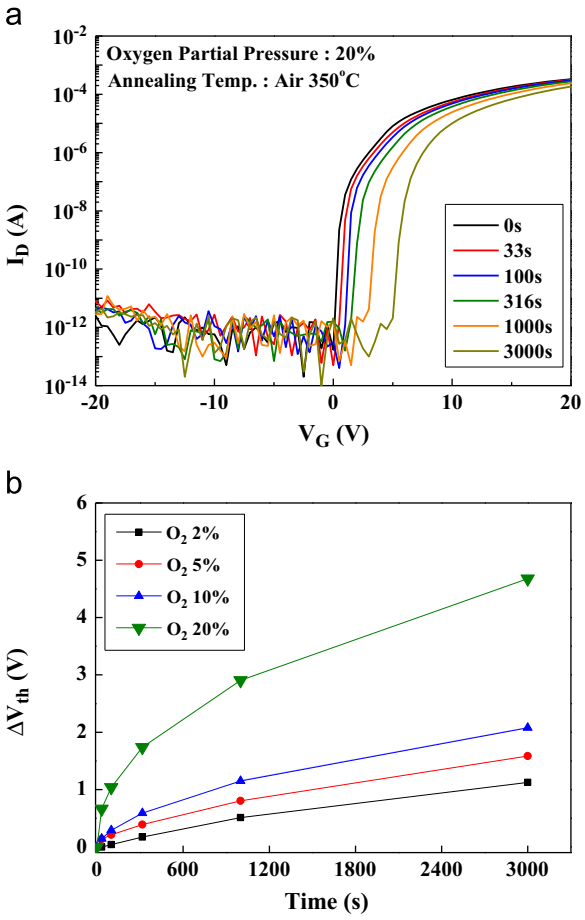

Fig. 3. (a) Evolution of transfer characteristics and (b) shift of threshold voltage under positive bias stress (+20 V) of GIGO TFTs.

considering the chemical bonding states and electronic structure, including the band alignment and band edge states below the conduction band.

First, the chemical bonding states were analyzed by XPS, and changes in the O 1s spectra are depicted in Fig. 4(a). The XPS spectra were collected after eliminating the surface contamination by adsorbed OH, C, H_2O, etc., and minimizing the preferred sputtering of light elements, using Ne ions at 500 eV. In order to differentiate the detailed oxygen states, the O 1s spectra were carefully deconvoluted into three peaks (O1, O2, O3), using Gaussian fitting along with subtraction of the Shirley type background [16]. The low binding energy peak (O1) at 530.7 eV is related to the O^{2-} ions on metal oxides, indicating Ge–In–Ga–O bonds [17]. The higher binding energy peak (O3) at around 532.6 eV is usually attributed to chemisorbed or dissociated oxygen or OH species on the surface of the GIGO film, such as $-CO_3$, adsorbed H_2O, or adsorbed O_2. On the other hand, the corresponding peak at intermediate binding energy (O2) of the O 1s spectrum is associated with OH bonding species and with O^{2-} ions that are in the oxygen-deficient Ge–In–Ga–O bonding matrix [18]. As shown in the relative ratio of the O2 peak ($O2/O_{total}$) of Fig. 4(b), the density of oxygen deficient bonding states (O2) slightly decreases even upon a decrease of oxygen partial pressure, indicating the strong oxygen bonding ability of Ge atoms [19].

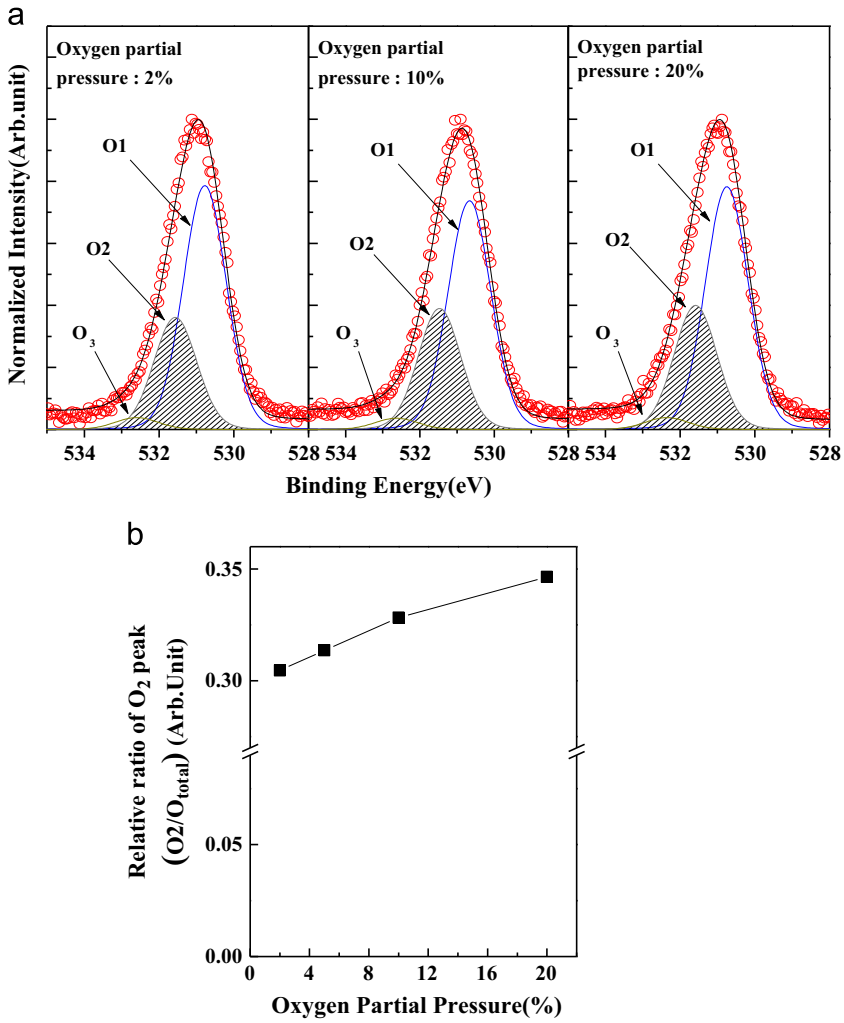

Fig. 4. (a) XPS spectra of O 1s core level and (b) relative ratio of O2 peak ($O2/O_{total}$) as a function of oxygen partial pressure.

Next, the valence band spectra were measured by a XPS analysis using the extrapolation method, as shown in Fig. 5(a). The bandgap (E_g) was also extracted using a SE analysis, and the relative energy differences (valence band offset (ΔE_{VB}): between the Fermi level (E_F) and valence band maximum, conduction band offset (ΔE_{CB}): between E_F and the conduction band minimum) are summarized in Fig. 5(b). Based on these values, a schematic energy band diagram of the GIGO film as a function of oxygen partial pressure is depicted in Fig. 5(b). The values of the extracted bandgap are similar, falling in a range of 3.60–3.67 eV, regardless of the oxygen partial pressure, but the ΔE_{VB} is decreased from 3.16 eV to 2.93 eV with an increase of oxygen partial pressure. As a result, the ΔE_{CB} shifts far from the conduction band minimum, from 0.44 eV ($pO_2=2\%$) to 0.74 eV ($pO_2=20\%$). This result is strongly corroborated with the decrease of carrier concentration and could be the plausible origin of degraded device operation with reduced mobility.

In order to further investigate the electronic structure of the GIGO films, including the band edge states below the conduction band, SE data were characterized as a function of oxygen partial pressure. Fig. 6(a) shows the imaginary dielectric function (ε_2) spectra from SE measurements for the GIGO films with the deconvoluted Gaussian band edge states ($D1$, $D2$), given by a simple four-phase model comprised of a Si substrate, SiO_2 overlayer, GIGO overlayer, and ambient layer. It has been suggested that $D1$ causes generation of carriers and $D2$ results in an increase of charge scattering/trapping, and thus, degradation of the mobility and stability [20,21]. As the oxygen partial pressure increased, the evolution of band edge states indicate that the shallow band edge state ($D1$) is slightly decreased, while the deep band edge state ($D2$) is drastically increased. This may be related to an increase of oxygen deficient chemical bonding states, such as oxygen vacancies [22]. Therefore, the GIGO film deposited at higher oxygen partial pressure ($pO_2=20\%$) is surmised to have a smaller carrier concentration, smaller mobility, and larger carrier trapping because of the decrease of shallow ($D1$) and the increase of deep ($D2$) band edge states. Also, from Fig. 6(c), it is noted that the relative energy positions of $D1$ and $D2$ shift to deeper levels from the conduction band minimum with an increase of oxygen partial pressure (i.e., $D1$: 0.19 eV→0.36 eV, $D2$: 0.68 eV→0.81 eV). These shifts to deeper energy levels of $D1$ and $D2$ within the bandgap could lead

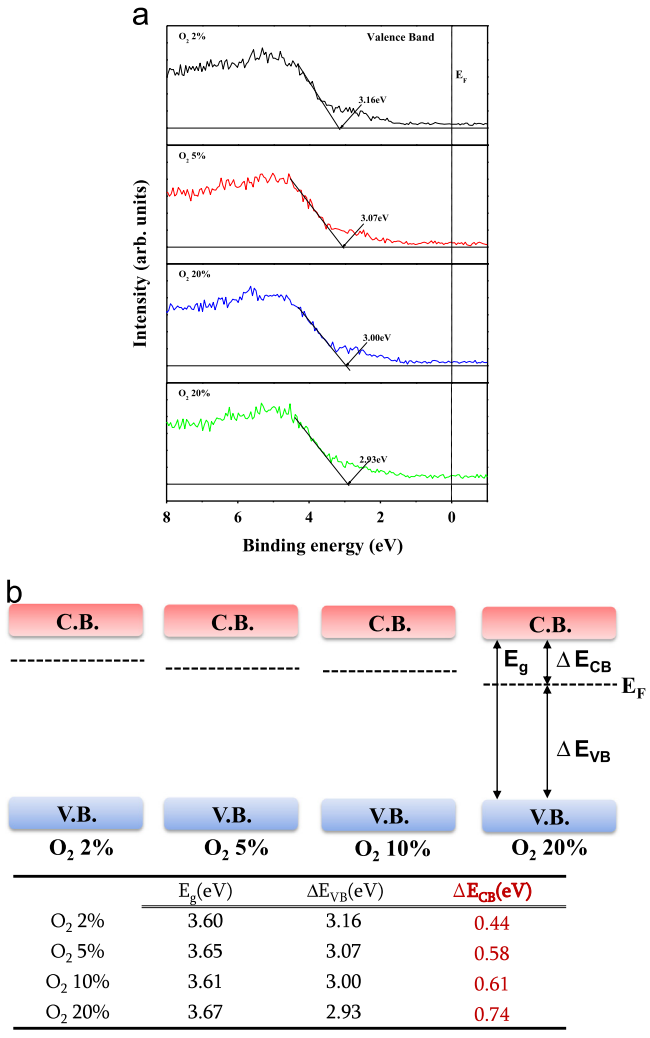

	E_g(eV)	ΔE_{VB}(eV)	ΔE_{CB}(eV)
O_2 2%	3.60	3.16	0.44
O_2 5%	3.65	3.07	0.58
O_2 10%	3.61	3.00	0.61
O_2 20%	3.67	2.93	0.74

Fig. 5. (a) XPS spectra near valence band and (b) schematic energy level diagram reflecting the relative energy position of the Fermi level (E_F) with respect to the conduction band minimum (CB) and valence band maximum (VB) as a function of oxygen partial pressure. The obtained values of the bandgap (E_g) and the relative energy difference between E_F and valence band (ΔE_{VB}) and between E_F and conduction band (ΔE_{CB}).

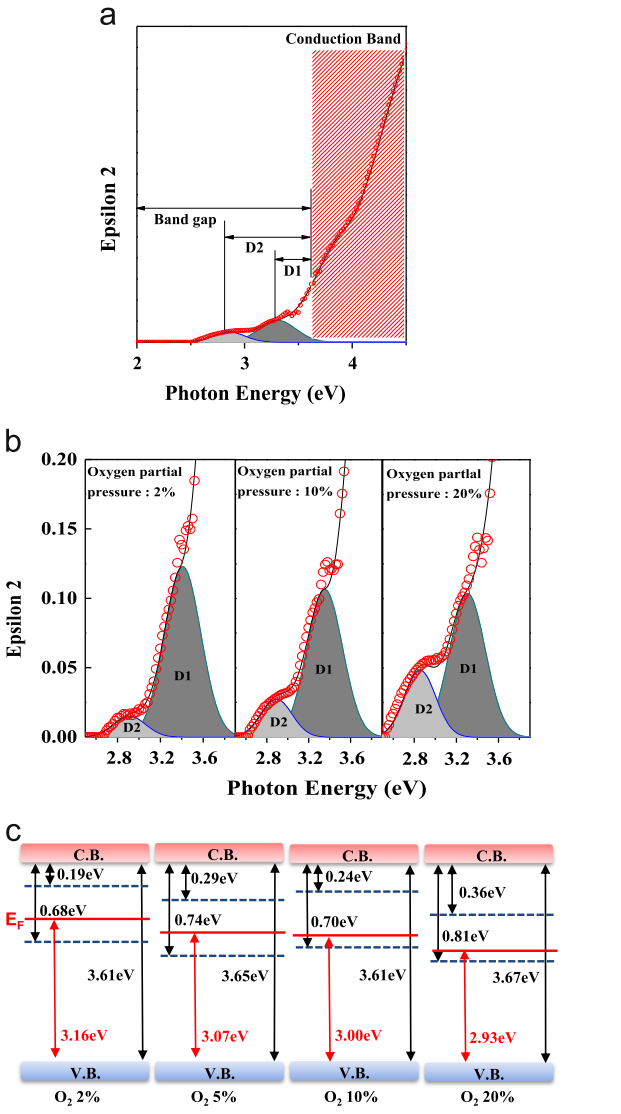

Fig. 6. (a) Imaginary dielectric function spectra from SE measurements for the GIGO film. Two distinct deconvoluted peaks, labeled *D*1 and *D*2, are Gaussian fits and represent the band edge states located below the conduction band edge. The band edge states are depicted as a function of oxygen partial pressure (2%, 10%, and 20%). (b) Schematic energy level diagram reflecting the energy level of band edge states (*D*1 and *D*2), as a function of oxygen partial pressure (2%, 10%, and 20%).

to larger degradation of device performance and stability, by increased in charge scattering/trapping during carrier transport due to the energy level far from the conduction band, rather than to an increase of carrier concentration, coupled with the relative position of the Fermi level and oxygen deficient bonding states. Therefore, as the oxygen partial pressure increased during the active deposition, the oxygen related states may be changed such that they not only shift from shallow-level (*D*1: donor-like) to deep-level (*D*2: accept-like) states, but also the amount of deep-level states is increased because of severe ion bombardment-damage [23] and oxygen-rearrangement [24] of the active layers.

4. Conclusions

We investigated the device performance and bias instability of GeInGaO oxide TFTs as a function of RF sputtered oxygen partial pressure. The TFT performances with the GIGO active layer deposited at lower oxygen pressure were significantly improved with a high field effect mobility of (14.46 cm^2/V s) and small threshold voltage within 1.5 V. It was revealed that the GIGO film deposited at lower oxygen pressure has a smaller conduction band offset ($\Delta E_{CB} = E_g - \Delta E_{VB}$) and smaller deep band edge states (*D*2) below the conduction band, which is related to oxygen deficient bonding states. In addition, with an increase of oxygen partial pressure the band edge states are shifted to deeper energy levels from the conduction band minimum. It was demonstrated that these evolutions of the electronic structure, such as the band alignment and band edge states of GIGO film, are strongly correlated to the device characteristics of GIGO TFTs, and are dependent on the oxygen partial pressure.

Acknowledgment

This research was partially supported by the Basic Science Research Program through the National Research Foundation of Korea (NRF), funded by the Ministry of Education, Science and Technology (No. 2012011730). This work was partially supported by the IT R&D Program of MKE/KETI (Grant no. 10041416, the core technology development of light and space adaptable new mode display for energy saving on 7 in. and 2 W) and by the MSIP (Ministry of Science, ICT & Future Planning) under the ITRC Support Program NIPA-2013-(H0301-13-1004) supervised by the NIPA.

References

[1] K. Nomura, H. Ohta, K. Ueda, T. Kamiya, M. Hirano, H. Hosono, Thin-film transistor fabricated in single-crystalline transparent oxide semiconductor, Science 300 (2003) 1269–1272.
[2] E. Fortunato, P. Barquinha, A. Pimentel, A. Goncalves, A. Marques, L. Pereira, R. Martins, Fully transparent ZnO thin-film transistor produced at room temperature, Advanced Materials 17 (2005) 590–594.
[3] K. Nomura, H. Ohta, A. Takagi, T. Kamiya, M. Hirano, H. Hosono, Room-temperature fabrication of transparent flexible thin-film transistors using amorphous oxide semiconductors, Nature 432 (2004) 488–492.
[4] J.Y. Kwon, K.S. Son, J.S. Jung, T.S. Kim, M.K. Ryu, K.B. Park, B.W. Yoo, J.W. Kim, Y.G. Lee, K.C. Park, S.Y. Lee, J.M. Kim, Bottom-gate gallium indium zinc oxide thin-film transistor array for high-resolution AMOLED display, IEEE Electron Device Letters 29 (2008) 1309–1311.
[5] J.S. Park, K. Kim, Y. Park, Y. Mo, H.D. Kim, J.K. Jeong, Novel ZrInZnO thin-film transistor with excellent stability, Advanced Materials 21 (2009) 329–333.
[6] R.A. Street, Thin-film transistors, Advanced Materials 21 (2009) 2007–2022.
[7] J.S. Park, W.J. Maeng, H.-S. Kim, J.-S. Park, Review of recent developments in amorphous oxide semiconductor thin-film transistor devices, Thin Solid Films 520 (2012) 1679–1693.
[8] K. Ghaffarzadeh, A. Nathan, J. Robertson, S. Kim, S. Jeong, C. Kim, U. Chung, J. Lee, Persistent photoconductivity in Hf–In–Zn–O thin film transistors, Applied Physics Letters 97 (2010) 143510.
[9] B.S. Yang, M.S. Hur, S. Oh, U.S. Lee, Y.J. Kim, M.S. Oh, J.K. Jeong, C.S. Hwang, H.J. Kim, Role of ZrO_2 incorporation in the suppression of negative bias illumination-induced instability in Zn–Sn–O thin film transistors, Applied Physics Letters 98 (2011) 122110.
[10] R.B.M. Cross, M.M. De Souza, Investigating the stability of zinc oxide thin film transistors, Applied Physics Letters 89 (2006) 263513.
[11] T. Kamiya, K. Nomura, H. Hosono, Subgap states, doping and defect formation energies in amorphous oxide semiconductor a-$InGaZnO_4$ studied by density functional theory, Physica Status Solidi A 207 (2010) 1698–1703.
[12] J.S. Park, J.K. Jeong, Y.G. Mo, H.D. Kim, C.J. Kim, Control of threshold voltage in ZnO-based oxide thin film transistors, Applied Physics Letters 93 (2008) 033513.
[13] J.H. Jeong, H.W. Yang, J.S. Park, J.K. Jeong, Y.G. Mo, H.D. Kim, J.W. Song, C.S. Hwang, Origin of subthreshold swing improvement in amorphous indium gallium zinc oxide transistors, Electrochemical and Solid-State Letters 11 (2008) H157–H159.
[14] W. Chen, S. Lo, S. Kao, H. Zan, C. Tsai, J. Lin, C. Fang, C. Lee, Oxygen-dependent instability and annealing/passivation effects in amorphous In–Ga–Zn–O thin-film transistors, IEEE Electron Device Letters 32 (2011) 1552–1554.
[15] S.Y. Park, K.H. Ji, H.Y. Jung, J.I. Kim, R.N. Choi, K.S. Son, M.K. Ryu, S.Y. Lee, J.K. Jeong, Improvement in the device performance of tin-doped indium oxide transistor by oxygen high pressure annealing at 150 °C, Applied Physics Letters 100 (2012) 162108.
[16] B.D. Ahn, J.H. Lim, M.-H. Cho, J.-S. Park, K.-B. Chung, Thin-film transistor behaviour and the associated physical origin of water-annealed In–Ga–Zn oxide semiconductor, Journal of Physics D 45 (2012) 415307.
[17] M. Chen, Z.L. Pei, C. Sun, L.S. Wen, X. Wang Jr., Surface characterization of transparent conductive oxide Al-doped ZnO films, Journal of Crystal Growth 220 (2000) 254–262.
[18] K.-C. Ok, J. Park, J.H. Lee, B.D. Ahn, J.H. Lee, K.-B. Chung, J.-S. Park, Semiconducting behavior of niobium-doped titanium oxide in the amorphous state, Applied Physics Letters 100 (2012) 142103.
[19] W.M. Haynes, CRC Handbook of Chemistry and Physics, 93rd ed., CRC, Boca Raton, Florida, 2012.
[20] H.-W. Park, J.-S. Park, J.H. Lee, K.-B. Chung, Thermal evolution of band edge states in ZnO film as a function of annealing ambient atmosphere, Electrochemical and Solid-State Letters 15 (2012) H133–H135.
[21] H.-W. Park, B.-K. Kim, J.-S. Park, K.-B. Chung, Device performance and bias instability of Ta doped InZnO thin film transistor as a function of process pressure, Applied Physics Letters 102 (2013) 102102.
[22] H. Seo, C.-J. Park, Y.-J. Cho, Y.-B. Kim, D.-K. Choi, Correlation of band edge native defect state evolution to bulk mobility changes in ZnO thin films, Applied Physics Letters 96 (2010) 232101.
[23] S. Kim, Y.W. Jeon, Y. Kim, D. Kong, H.K. Jung, M. Bae, J. Lee, B.D. Ahn, S.Y. Park, J.-H. Park, J. Park, H.-I. Kown, D.M. Kim, D. H. Kim, Impact of oxygen flow rate on the instability under positive bias stresses in DC-sputtered amorphous InGaZnO thin-film transistors, IEEE Electron Device Letters 33 (2012) 62–64.
[24] M. Furuta, Y. Kamada, M. Kimura, T. Hiramatsu, T. Matsuda, H. Furuta, C. Li, S. Fujita, T. Hirao, Analysis of hump characteristics in thin-film transistors with ZnO channels deposited by sputtering at various oxygen partial pressures, IEEE Electron Device Letters 31 (2010) 1257–1259.